Parametric decay of Alfvén waves in multicomponent plasmas

G. Gnavi,[1] R. M. O. Galvão,[2] F. T. Gratton,[1] and L. Gomberoff[3]
[1]*Instituto de Física del Plasma, Consejo Nacional de Investigaciones Científicas y Técnicas and Departamento de Física, Universidad de Buenos Aires, Ciudad Universitaria, Pab. 1, 1428 Buenos Aires, Argentina*
[2]*Instituto de Física, Universidade de São Paulo, C.P. 66318, 05389-970, São Paulo, São Paulo, Brazil*
[3]*Departamento de Física, Facultad de Ciencias, Universidad de Chile, Casilla 653, Santiago, Chile*
(Received 20 November 1995)

The parametric couplings of a finite amplitude Alfvén wave in a multicomponent plasma are investigated including the effect of damping. The important case of a fusion plasma with deuterium, tritium, and α particle ions, heated by neutral beam injection, is analyzed in detail. Because of the modification in the linear dispersion relation caused by the drifting ions, there appear many couplings to sound waves and an electromagnetic modulational instability. The threshold on the pump amplitude is determined as a function of the damping rates. The relevance of our results to the stability of toroidal Alfvén eigenmodes in tokamaks is discussed. [S1063-651X(96)01909-5]

PACS number(s): 52.35.Bj, 52.35.Fp, 52.55.Pi

I. INTRODUCTION

The decay of large amplitude Alfvén and ion cyloctron waves by nonlinear coupling with sound waves and other modes has been studied for a long time (See, e.g., Refs. [1–6]). Recently, this subject has received attention in two different areas. Firstly, it was recognized that nonlinear coupling may play a quite important role in the saturation of toroidal eigenmodes (TAE's) in tokamak fusion reactors, reducing their potential danger for the achievement of ignition [7–11]. On the other hand, space physicists realized that the presence of drifting species in multicomponent plasmas affects strongly the linear and nonlinear stability of ion cyclotron and Alfvén waves, modifying substantially the picture of physical processes that are relevant for the heating and acceleration of particles in the solar wind [12–14]. The research related to the saturation of TAE's has been concentrated on the coupling between magnetohydrodynamic modes assuming that a broad spectrum may be excited [7–11]. Although in all these works kinetic and toroidal effects are taken into account, the influence of different species, including drifting ones, which are present in fusion plasmas heated by neutral beam injection, has not been considered. In space plasmas the geometry is rather simple and the presence of many ionic species can be readily included in the model. However, the study of parametric instabilities in this context has been carried out without including damping, which is very important for sound waves and for the daughter electromagnetic waves when their frequency is close to the resonance of an ion component. The sound waves in fusion plasmas may be not heavily damped, in particular the ones supported mainly by a drifting species; but the daughter Alfvén waves may occur close to the continuum and be strongly damped. Therefore, in both areas the inclusion of damping is essential to calculate the corresponding thresholds on the pump amplitude and to evaluate the relevance of the various parametric processes.

In this paper we investigate the parametric couplings of ion-cyclotron and Alfvén waves with sound waves in multicomponent plasmas described by fluid equations including collisional damping to model the effect of kinetic and continuum damping. We consider waves propagating in the direction of a constant magnetic field in an uniform plasma. Our formulas are directly applicable to space plasmas. Although our calculations do not include toroidal and kinetic effects, they can also be considered as a first step towards the evaluation of some processes affecting the decay of TAE's in fusion plasmas that have not been taken into account so far. The dispersion relation for the parametric instabilities is derived in the next section. We follow an approach that preserves the structure of the linear dielectric tensor, making it easier to introduce the influence of different physical mechanisms, in particular collisional damping, than in derivations available in the recent literature [13–17]. Collisions are considered as a first order effect and, therefore, are kept in the linear part of the dielectric tensor only. We use a Krook model with different collision frequencies for the various species. Landau and continuum damping can be mocked up by properly choosing the values of the different collision frequencies. The numerical solutions of the dispersion relation are presented in Sec. III for the case of an Alfvén wave in a fusion plasma scenario. The presence of many ion species, drifting ones in particular, with their associated sound wave branches, opens up many channels for parametric couplings. The saturation of TAE modes by mode coupling has been considered by different authors. Hahm and Chen have studied a many mode process in the random phase approximation [9]. Saturation occurs due to energy transfer down to smaller wavelengths and eventually damping into the continuum. Vlad and co-workers have investigated a nonlinear magnetohydrodynamics (MHD) process in which the interaction between two modes leads to a modification of the equilibrium poloidal field such that the gap in the continuum Alfvén spectrum is altered, causing a frequency shift and, therefore, saturation [11]. The beat between two Alfvén waves has also been considered by Gang and Leboeuf [10]. It is interesting to note that the saturation amplitudes encountered in these works are all of the same order, viz., $\tilde{B}_r/B_z$ of the order of a few percent, where $\tilde{B}_r$ is the radial component of the perturbed magnetic field and B_z the equilibrium mag-

netic field. It is important to stress that the process that we consider here is rather different, i.e., coherent mode coupling between electromagnetic and sound waves in the presence of collisional damping. As we show in the numerical calculations, this mechanism may be relevant for amplitudes of the perturbation also of the order of a few percent.

Continuum damping of the Alfvén wave and Landau damping of the sound wave are simulated by the inclusion of a collision frequency in the corresponding linear terms of the dispersion relation. We find that a threshold for the parametric process occurs only if the electromagnetic daughter wave is damped. Otherwise, if one assumes that the daughter wave is unstable, which corresponds to a negative collision frequency, there is no threshold independent of the damping of the sound wave. Discussions and conclusions are presented in the last section.

II. DISPERSION RELATION

Let us first briefly review the derivation of the dispersion relation for electromagnetic ion cyclotron waves (EICW) propagating along the external magnetic field B_z in an uniform plasma. The equation of motion for each species is given by

$$m_s\left(\frac{\partial \mathbf{V}_s}{\partial t}+V_{zs}\frac{\partial \mathbf{V}_s}{\partial z}\right)=q_s\left(\mathbf{E}+\frac{1}{c}\mathbf{V}_s\times\mathbf{B}\right)-\frac{\nabla p_s}{n_s}, \quad (1)$$

where $\mathbf{E}$ and $\mathbf{B}$ are the electric and magnetic fields, $\mathbf{V}_s$, q_s, m_s, and n_s are the velocity, charge, mass, and density of species s, respectively, p_s is the pressure, and c is the speed of light (cgs units are used throughout). We assume that the unperturbed plasma is quasineutral and current free. Representing the fields of the circularly polarized waves by $B_\perp=B_x+iB_y=B\exp(ik_0z-i\omega_0t)$ and $E_\perp=E_x+iE_y=-iE\exp(ik_0z-i\omega_0t)$, we solve Eq. (1) taking $V_{\perp s}=V_{xs}+iV_{ys}=V^0_{\perp s}\exp(ik_0z-i\omega_0t)$. Combining Eq. (1) with Maxwell's equations, we obtain the dispersion relation for low-frequency EICW, that is,

$$k_0^2=\frac{4\pi}{B_z^2}\sum_j\frac{m_jn_j(\omega_0-k_0V_j)^2}{[1-(\omega_0-k_0V_j)/\Omega_j]}, \quad (2)$$

where V_j and $\Omega_j=q_jB_z/m_jc$ are the zero-order drift speed (in the z direction) and cyclotron frequency of ion species j, respectively. In deriving Eq. (2), we have taken the limit $m_e\to0$, and the sum on the right-hand side is over ion species only.

The dispersion relation is valid for finite amplitude ion-cyclotron waves. We consider one such wave as the ''pump'' wave. To investigate the nonlinear couplings, the wave-plasma system is then perturbed by including small amplitude longitudinal sound waves with wave number k and frequency ω, i.e., $\delta V_{zs}=\mathrm{Re}[\delta u_s\exp(ikz-i\omega t)]$, $\delta E_z=\mathrm{Re}[\delta\mathcal{E}\exp(ikz-i\omega t)]$, and $\delta n_s=\mathrm{Re}[\delta\tilde{n}_s\exp(ikz-i\omega t)]$. From the equation of continuity, we obtain

$$\delta n_s=n_s\mathrm{Re}\left[\frac{k\delta u_s}{\omega_s}\exp(ikz-i\omega t)\right], \quad (3)$$

with $=\omega_s=\omega-kV_s$. For adiabatic perturbations, pressure and density are related by $\delta p_s/p_s=\gamma_s\delta n_s/n_s$, where γ_s is the ratio of specific heats.

In the following we will derive the complete dispersion relation for the coupled waves in a way in which the nonlinear contribution to the plasma dielectric tensor is explicitly shown. We will present the derivation of the dispersion relation for a collisionless plasma. The effect of collisions can then be included by modifying the linear part of the dispersion relation.

The coupling of the sound waves with the pump wave excites the daughter waves with wave numbers $k_\pm=k_0\pm k$ and frequencies $\omega_\pm=\omega_0\pm\omega$. We define, accordingly,

$$\delta E_\perp=\delta E_+\exp(ik_+z-i\omega_+t)+\delta E^*_-\exp(ik^*_-z-i\omega^*_-t), \quad (4)$$

$$\delta B_\perp=\delta B_+\exp(ik_+z-i\omega_+t)+\delta B^*_-\exp(ik^*_-z-i\omega^*_-t), \quad (5)$$

$$\delta V_{\perp s}=\delta v_{+s}\exp(ik_+z-i\omega_+t)+\delta v^*_{-s}\exp(ik^*_-z-i\omega^*_-t), \quad (6)$$

$$\delta j_{\perp s}=\delta j_{+s}\exp(ik_+z-i\omega_+t)+\delta j^*_{-s}\exp(ik^*_-z-i\omega^*_-t). \quad (7)$$

For low frequency waves the electrons can be considered massless, so that the left-hand side (LHS) of Eq. (1) for electrons is equal to zero. The perpendicular components give

$$c\,\delta E_\perp-i(B_z\delta v_{\perp e}-V_e\delta B_\perp-B_\perp\delta u_e)=0 \quad (8)$$

(V_e, drift speed of electrons) and the parallel component is

$$c\,\delta E_z+\mathrm{Im}\{V^{0*}_{\perp e}\delta B_\perp+B_\perp\delta v^*_{\perp e}\}+\frac{c}{en_e}\gamma_eKT_e\frac{\partial}{\partial z}\delta n_e=0. \quad (9)$$

The equation of continuity, Eq. (3), gives a link between δu_e and $\delta\tilde{n}_e$, $\delta u_e=\omega_e\delta\tilde{n}_e/kn_e$. Thus, one can obtain $\delta v_{\perp e}$ and δn_e as functions of the electric and magnetic fields from Eqs. (8) and (9).

An expression for the electron current can be derived from Eq. (8),

$$\delta j_{\pm e}=\frac{cen_e}{B_z}\left[i\omega_{\pm e}\delta E_\pm-\frac{B}{2c}\left(\frac{\omega}{k}-\frac{\omega_0}{k_0}\right)\frac{k\delta u_e}{\omega_e}\right], \quad (10)$$

where $\omega_{\pm e}=\omega_\pm-V_ek_\pm$. There may exist several groups of electrons in the plasma, with different densities and drift velocities. However, as we shall see immediately, under the conditions we set here, a detailed specification of these electron populations is not necessary. In fact, the total electron current contribution does not depend explicitly on the value of the electron drifts. A sum of Eq. (10) over all possible electron groups leads to

$$\sum_e\delta j_{\pm e}=\frac{1}{B_z}\left[\frac{(\pm i)}{\omega_\pm}\left(\omega_\pm\sum_e en_e-k_\pm\sum_e en_eV_e\right)\delta E_\pm-\frac{B}{2}\left(\frac{\omega}{k}-\frac{\omega_0}{k_0}\right)\sum_e e\delta\tilde{n}_e\right]. \quad (11)$$

As we can see only the total zero order electron current enters in Eq. (11), and we assume that the configuration is current free, so that $\Sigma e n_e V_e$ is balanced by the total longitudinal zero order ion current. Similarly, due to charge neutrality, $\Sigma e n_e$ is balanced by the total zero order ion charge density. Therefore, the first two terms on the right-hand side (RHS) of Eq. (11) are canceled by similar contributions of the total ion current, $\Sigma \delta j_{\pm j}$. In addition, the range of frequencies considered here allows us to apply the quasineutrality approximation; i.e., $\Sigma e \delta \tilde{n}_e$ is balanced by the ion charge perturbation. Hence, also the third term on the RHS of Eq. (11) is eliminated by a corresponding ion contribution if Poisson's equation is replaced by the charge neutrality condition,

$$4\pi \sum_j q_j n_j \frac{\delta u_j k}{\omega_j} = 4\pi \sum e \delta \tilde{n}_e . \tag{12}$$

The RHS of this equation is computed from

$$\frac{\delta \tilde{n}_e}{n_e} = \frac{ie}{k \gamma_e K T_e} \left[\delta \mathcal{E} + \frac{B}{B_z} (C^+ \delta E_+ + C^- \delta E_-) \right] \tag{13}$$

[which follows from Eqs. (8) and (9) by eliminating $\delta v_{\perp e}$], where

$$C^{\pm} = 1 - k_{\pm} \omega_0 / \omega_{\pm} k_0 .$$

We note, as commented above, that $\delta \tilde{n}_e$ does not depend on any particular value of the electron drift velocities, V_e. Finally, the total perturbed electron charge density that enters in Eq. (12) is given by

$$4\pi \sum_e e \delta \tilde{n}_e = \frac{i}{k} \left[\delta \mathcal{E} + \frac{B}{B_z} (C^+ \delta E_+ + C^- \delta E_-) \right] \sum_e \frac{4\pi e^2 n_e}{\gamma_e K T_e} . \tag{14}$$

In the preceding equation we are admitting the presence of electron populations with different temperatures.

We can now focus our attention on the ion dynamics. We obtain from Eq. (1)

$$\delta v_{\pm j} = \frac{1}{B_z A_{\pm j}} \left(\frac{B}{2A_{0j}} \delta u_j - \frac{\omega_{\pm j}}{k_{\pm}} \delta B_{\pm} \right), \tag{15}$$

and

$$\left(1 - \frac{k^2 \gamma_j v_{Sj}^2}{\omega_j^2} \right) \delta u_j = \frac{q_j}{m_j \omega_j} \left[i \delta \mathcal{E} + \frac{B}{c} \left(\frac{\omega_{0j}}{k_0 B_z A_{0j}} (\delta B_- - \delta B_+) + \delta v_{-j} - \delta v_{+j} \right) \right], \tag{16}$$

where $v_{Sj}^2 \equiv p_j / n_j m_j$ is the square of the thermal speed of the jth species, $\omega_{0j} \equiv \omega_0 - V_j k_0$, $\omega_{\pm j} = \omega_{\pm} - V_j k_{\pm}$, $A_{0j} \equiv 1 - (\omega_{0j}/\Omega_j)$, and $A_{\pm j} \equiv 1 - (\omega_{\pm j}/\Omega_j)$. Eliminating the δv's from Eq. (15), and using Faraday's law, $\omega_{\pm} \delta B_{\pm} = \pm i c k_{\pm} \delta E_{\pm}$, we find that

$$\delta u_j = \frac{ic\Omega_j}{\omega_j S_j} \left[\frac{1}{B_z} \delta \mathcal{E} + \frac{B}{B_z^2} (C_j^+ \delta E_+ + C_j^- \delta E_-) \right], \tag{17}$$

where

$$S_j \equiv 1 - \frac{\gamma_j v_{Sj}^2 k^2}{\omega_j^2} + \left(\frac{B}{B_z} \right)^2 \frac{1}{A_{0j} A_{+j} A_{-j}}, \tag{18}$$

$$C_j^{\pm} \equiv \frac{k_{\pm}}{\omega_{\pm}} \left(\frac{\omega_{\pm j}}{k_{\pm} A_{\pm j}} - \frac{\omega_{0j}}{k_0 A_{0j}} \right). \tag{19}$$

Since

$$\delta j_{\perp j} = q_j (n_{j0} \delta V_{\perp j} + V_{\perp j}^0 \delta n_j),$$

then

$$\delta j_{\pm j} = q_j n_j \left(\delta v_{\pm j} - \frac{B}{B_z} \frac{\omega_{0j} k}{2A_{0j} \omega_j k_0} \delta u_j \right). \tag{20}$$

Thus, from this relationship and Eq. (15), we can express the sum of ion contributions as

$$\begin{aligned} \sum_j \delta j_{\pm j} = \frac{\mp ic}{B_z \omega_{\pm}} & \left(\omega_{\pm} \sum_j q_j n_j - k_{\pm} \sum_j q_j n_j V_j \right. \\ & \left. + \frac{c}{B_z} \sum_j \frac{m_j n_j \omega_{\pm j}^2}{A_{\pm j}} \right) \delta E_{\pm} \\ & + \frac{cB}{2B_z^2} \sum_j \frac{m_j n_j}{A_{0j}} \left(\frac{\omega_{\pm j}}{A_{\pm j}} + \omega_{0j} - \frac{k \omega_{0j}^2}{k_0 \omega_j} \right) \delta u_j \\ & + \frac{B}{2B_z} \left(\frac{\omega}{k} - \frac{\omega_0}{k_0} \right) \sum_j q_j \delta \tilde{n}_j . \end{aligned} \tag{21}$$

Ampère's law neglecting the displacement current term is

$$c k_{\pm} \delta B_{\pm} = -4\pi \sum_j \delta j_{\pm j} - 4\pi \sum_e \delta j_{\pm e} . \tag{22}$$

We see that the perturbed electron current, Eq. (13), cancels the ion current terms in Eq. (21) that are independent of the ion mass. Therefore, Eq. (22) can be written as

$$\begin{aligned} \left[k_{\pm}^2 - \sum_j \frac{4\pi m_j n_j}{B_z^2 A_{\pm j}} \omega_{\pm j}^2 \right] \delta E_{\pm} = & \pm \frac{i}{2} \omega_{\pm} \sum_j \frac{4\pi m_j n_j}{B_z^2 A_{0j}} \\ & \times \left[\omega_{0j} - \frac{k \omega_{0j}^2}{k_0 \omega_j} + \frac{\omega_{\pm j}}{A_{\pm j}} \right] \\ & \times \frac{B}{c} \delta u_j , \end{aligned} \tag{23}$$

where the sums are over ions only. These relationships can be expressed as

$$(n_{\pm}^2 - L_{\pm}) \delta E_{\pm} = \pm \frac{i}{c} \sum_j \mathcal{R}_{\pm j} B \delta u_j , \tag{24}$$

with the following definitions:

$$n_{\pm}^2 \equiv \frac{c^2 k_{\pm}^2}{\omega_{\pm}^2}, \quad L_{\pm} \equiv \frac{4\pi c^2}{B_z^2} \sum_j \frac{m_j n_j}{A_{\pm j}} \frac{\omega_{\pm j}^2}{\omega_{\pm}^2}, \tag{25}$$

and

$$\mathcal{R}_{\pm j} \equiv \frac{c^2}{2\omega_{\pm}} \frac{4\pi m_j n_j}{B_z^2 A_{0j}} \left[\omega_{0j} - \frac{k\omega_{0j}^2}{k_0 \omega_j} + \frac{\omega_{\pm j}}{A_{\pm j}} \right]. \tag{26}$$

Taking into account the expressions for the δu_j's given by Eq. (17), and defining the parameter $\mathcal{A} \equiv B/B_z$, which measures the amplitude of the ''pump'' wave relative to the background magnetic field, we may write

$$\begin{aligned}(n_+^2 - L_+)\,\delta E_+ = &- \sum_j \left(\frac{\Omega_j \mathcal{R}_{+j} C_j^+}{\omega_j S_j} \right) \frac{B^2}{B_z^2}\, \delta E_+ \\ &- \sum_j \left(\frac{\Omega_j \mathcal{R}_{+j} C_j^-}{\omega_j S_j} \right) \frac{B^2}{B_z^2}\, \delta E_- \\ &- \sum_j \left(\frac{\Omega_j \mathcal{R}_{+j}}{\omega_j S_j} \right) \frac{B}{B_z}\, \delta \mathcal{E} \qquad (27)\end{aligned}$$

$$\equiv -\{\mathcal{A}^2 R_{++}\,\delta E_+ + \mathcal{A}^2 R_{+-}\,\delta E_- + \mathcal{A} R_{+\parallel}\,\delta \mathcal{E}\} \tag{28}$$

and

$$\begin{aligned}(n_-^2 - L_-)\,\delta E_- = &+ \sum_j \left(\frac{\Omega_j \mathcal{R}_{-j} C_j^+}{\omega_j S_j} \right) \frac{B^2}{B_z^2}\, \delta E_+ \\ &+ \sum_j \left(\frac{\Omega_j \mathcal{R}_{-j} C_j^-}{\omega_j S_j} \right) \frac{B^2}{B_z^2}\, \delta E_- \\ &+ \sum_j \left(\frac{\Omega_j \mathcal{R}_{-j}}{\omega_j S_j} \right) \frac{B}{B_z}\, \delta \mathcal{E} \qquad (29)\end{aligned}$$

$$\equiv \{\mathcal{A}^2 R_{-+}\,\delta E_+ + \mathcal{A}^2 R_{--}\,\delta E_- + \mathcal{A} R_{-\parallel}\,\delta \mathcal{E}\}. \tag{30}$$

In Eq. (28), the quantities R_{++}, R_{+-}, and $R_{+\parallel}$ represent the coefficients of $\mathcal{A}^2 \delta E_+$, $\mathcal{A}^2 \delta E_-$, and $\mathcal{A}\delta\mathcal{E}$ in Eq. (27), respectively. Similarly, in Eq. (30), the symbols R_{-+}, R_{--}, and $R_{\parallel}$ have the same meaning with respect to Eq. (29).

An equation for the longitudinal component may be derived from Eq. (12). It can be expressed as

$$\begin{aligned}\epsilon_\parallel \delta \mathcal{E} = &\left(\sum_j \frac{4\pi q_j^2 n_j C_j^+}{m_j \omega_j^2 S_j} - C^+ \sum_e \frac{4\pi e^2 n_e}{\gamma_e K T_e k^2} \right) \frac{B}{B_z}\, \delta E_+ \\ &+ \left(\sum_j \frac{4\pi q_j^2 n_j C_j^-}{m_j \omega_j^2 S_j} - C^- \sum_e \frac{4\pi e^2 n_e}{\gamma_e K T_e k^2} \right) \frac{B}{B_z}\, \delta E_- \qquad (31)\end{aligned}$$

$$\equiv \{\mathcal{A} R_{\parallel +}\,\delta E_+ + \mathcal{A} R_{\parallel -}\,\delta E_-\}, \tag{32}$$

with

$$\epsilon_\parallel = \sum_e \frac{4\pi e^2 n_e}{\gamma_e K T_e k^2} - \sum_j \frac{4\pi q_j^2 n_j}{m_j \omega_j^2 S_j}. \tag{33}$$

In the limit of zero pump intensity, $B=0$, Eqs. (27), (29), and (31) give the linear dispersion relations of sideband EICW's, $n_{\pm}^2 = L_{\pm}$, and sound waves $\epsilon_\parallel = 0$. The LHS of Eqs. (27), (29), and (31) corresponds to the linear approximation of the modes, and the RHS represents the coupling of the modes with the pump.

In matrix form, Eqs. (28), (30), and (32) become

$$\begin{pmatrix} n_+^2 - L_+ + \mathcal{A}^2 R_{++} & \mathcal{A}^2 R_{+-} & \mathcal{A} R_{+\parallel} \\ -\mathcal{A}^2 R_{-+} & n_-^2 - L_- - \mathcal{A}^2 R_{--} & -\mathcal{A} R_{-\parallel} \\ -\mathcal{A} R_{\parallel +} & -\mathcal{A} R_{\parallel -} & \epsilon_\parallel \end{pmatrix} \times \begin{pmatrix} \delta E_+ \\ \delta E_- \\ \delta \mathcal{E} \end{pmatrix} = 0 \tag{34}$$

The dispersion relation is thus given by

$$\begin{aligned}&(n_+^2 - L_+)(n_-^2 - L_-)\epsilon_\parallel + \mathcal{A}^2 \{(R_{s++}\epsilon_\parallel + R_{\parallel +} R_{+\parallel})(n_-^2 - L_-) \\ &\quad - (R_{--}\epsilon_\parallel + R_{\parallel -} R_{-\parallel})(n_+^2 - L_+)\} + \mathcal{A}^4 \{(R_{+-} R_{-+} \\ &\quad - R_{++} R_{--})\epsilon_\parallel + R_{+-} R_{\parallel +} R_{-\parallel} + R_{-+} R_{\parallel -} R_{+\parallel} \\ &\quad - R_{--} R_{\parallel +} R_{+\parallel} - R_{++} R_{\parallel -} R_{-\parallel}\} \\ &= 0. \qquad (35)\end{aligned}$$

We remark that no approximations have been made with respect to the strength of the pump in the derivation of the dispersion relation. In particular, the quantities S_j, Eq. (18), which appear in the definition of $\epsilon_\parallel$, have a term proportional to $\mathcal{A}^2$, i.e., to the square of the normalized pump amplitude, which can be significant for finite pump amplitude, and modify the propagation of the sound waves. This effect is not included, e.g., in Ref. [2] in view of the approximations adopted there. The coefficients $C_j^{\pm}$ are formed by variables corresponding to transverse waves only. Equation (35) contains all the parametric couplings predicted by a multifluid model and can be used to compute the growth rates of the processes.

The nonlinear dispersion relation, Eq. (35), which describes all the parametric instabilities generated by the EICW pump, does not contain damping effects and, therefore, does not give information about the thresholds of these instabilities. However, it is possible to modify the LHS of Eqs. (27), (29), and (31) to include heuristically simple collision corrections in the linear dielectric terms $L_{\pm}$ and $\epsilon_\parallel$. The rationale is that since the instability thresholds are expected at small values of $\mathcal{A}$, then the RHS of Eqs. (27), (29), and (31) are considered as corrections to the linear part. Therefore, the addition of a damping effect is included in the linear (LHS) terms only, while the RHS are maintained collisionless as before. In the dynamic equations of ions, Eq. (1), we add a term $-m_j \nu_j V_j$ in the RHS, where ν_j is a phenomenological collision frequency to model wave damping. Then, the linear equation $n_{\pm}^2 - L_{\pm} = 0$ for the sidebands becomes

$$(k_0\pm k)^2=\frac{4\pi}{B_z^2}\sum_j n_j m_j\,\frac{[\omega_0\pm\omega-(k_0\pm k)V_j][\omega_0\pm(\omega+i\nu_j)-(k_0\pm k)V_j]}{1-[\omega_0\pm(\omega+i\nu_j)-(k_0\pm k)V_j]/\Omega_j}, \tag{36}$$

which can be compared with Eq. (2) to see the changes introduced by the *ad hoc* collision term. A similar modification must be introduced in $\epsilon_\parallel$.

For the purpose of numerical analysis and applications, we introduce normalized variables using the cyclotron frequency Ω_1 and the Alfvén velocity, $v_A\equiv(B_z^2/4\pi n_1 m_1)^{1/2}$, of species $j=1$ as normalization values, following the notation of some recent literature [13,14]. The normalized quantities are then defined as, $\eta_j=n_j/n_1$, $\eta_e=n_e/n_1$, $\overline{m_j}=m_j/m_1$, $\overline{q_j}=q_j/q_1$, $X\equiv\omega/\Omega_1$, $Y\equiv kV_A/\Omega_1$, $X_0\equiv\omega_0/\Omega_1$, $Y_0\equiv k_0V_A/\Omega_1$, $U_j=V_j/V_A$, $X_j\equiv X-U_jY$, $X_{0j}\equiv X_0-U_jY_0$, $X_\pm\equiv X_0\pm X$, $Y_\pm\equiv Y_0\pm Y$, $X_{\pm j}\equiv X_\pm-U_jY_\pm$, $A_{0j}\equiv1-(\overline{m_j}/\overline{q_j})X_{0j}$, $A_{\pm j}\equiv1-(\overline{m_j}/\overline{q_j})X_{\pm j}$, $\beta_j\equiv m_j v_{Sj}^2/m_1v_A^2$, and $\beta_e\equiv\gamma_eKT_e/m_1v_A^2$. The following relationships hold:

$$\begin{aligned}D_+\delta E_+&=-\{\mathcal{A}^2R_{++}\delta E_++\mathcal{A}^2R_{+-}\delta E_-+\mathcal{A}R_{+\parallel}\delta\mathcal{E}\}\\&\equiv-\sum_j\left\{\left(\frac{\overline{q_j}\mathcal{R}_{+j}\overline{C_j^+}}{\overline{m_j}X_jS_j}\right)\frac{B^2}{B_z^2}\,\delta E_++\left(\frac{\overline{q_j}\mathcal{R}_{+j}\overline{C_j^-}}{\overline{m_j}X_jS_j}\right)\right.\\&\left.\times\frac{B^2}{B_z^2}\,\delta E_-+\left(\frac{\overline{q_j}\mathcal{R}_{+j}}{\overline{m_j}X_jS_j}\right)\frac{B}{B_z}\,\delta\mathcal{E}\right\},\end{aligned} \tag{37}$$

$$\begin{aligned}D_-\delta E_-&=\{\mathcal{A}^2R_{-+}\delta E_++\mathcal{A}^2R_{--}\delta E_-+\mathcal{A}R_{-\parallel}\delta\mathcal{E}\}\\&\equiv\sum_j\left\{\left(\frac{\overline{q_j}\mathcal{R}_{-j}\overline{C_j^+}}{\overline{m_j}X_jS_j}\right)\frac{B^2}{B_z^2}\,\delta E_++\left(\frac{\overline{q_j}\mathcal{R}_{-j}\overline{C_j^-}}{\overline{m_j}X_jS_j}\right)\right.\\&\left.\times\frac{B^2}{B_z^2}\,\delta E_-+\left(\frac{\overline{q_j}\mathcal{R}_{-j}}{\overline{m_j}X_jS_j}\right)\frac{B}{B_z}\,\delta\mathcal{E}\right\},\end{aligned} \tag{38}$$

and

$$\begin{aligned}d_\parallel\delta\mathcal{E}&=\mathcal{A}R_{\parallel+}\delta E_++\mathcal{A}R_{\parallel-}\delta E_-\\&\equiv\frac{B}{B_z}\left\{\left[\sum_j\frac{\eta_j\overline{q_j^2}\overline{C_j^+}Y^2}{\overline{m_j}X_j^2S_j}-\frac{1}{\overline{\beta_e}}\overline{C^+}\right]\delta E_+\right.\\&\left.+\left[\sum_j\frac{\eta_i\overline{q_j^2}\overline{C_j^-}Y^2}{\overline{m_j}X_j^2S_j}-\frac{1}{\overline{\beta_e}}\overline{C^-}\right]\delta E_-\right\},\end{aligned} \tag{39}$$

with

$$D_\pm=\frac{Y_\pm^2}{X_\pm^2}-\sum_j\frac{\eta_j\overline{m_j}}{\overline{A_{\pm j}}}\frac{X_{\pm j}^2}{X_\pm^2}, \tag{40}$$

$$D_\parallel=\left\{\frac{1}{\overline{\beta_e}}-\sum_j\frac{\eta_j\overline{q_j^2}Y^2}{\overline{m_j}X_j^2S_j}\right\}, \tag{41}$$

$$\mathcal{R}_{\pm j}=\frac{1}{X_\pm}\frac{\eta_j\overline{m_j}}{2A_{0j}}\left[X_{0j}-\frac{YX_{0j}^2}{Y_0X_j}+\frac{X_{\pm j}}{\overline{A_{\pm j}}}\right], \tag{42}$$

$$\overline{C^{\pm j}}=\frac{Y_\pm}{X_\pm}\left(\frac{X_{\pm j}}{Y_\pm\overline{A_{\pm j}}}-\frac{X_{0j}}{Y_0\overline{A_{0j}}}\right), \tag{43}$$

$$\overline{C^\pm}=1-\frac{Y_\pm X_0}{Y_0X_\pm}, \tag{44}$$

$$S_j=1-\frac{\beta_j}{\overline{m_j}}\frac{Y^2}{X_j^2}+\mathcal{A}^2\frac{1}{\overline{A_{0j}}\,\overline{A_{+j}}\,\overline{A_{-j}}}, \tag{45}$$

$$\frac{1}{\overline{\beta_e}}=\frac{e}{q_1}\sum_e\frac{n_e}{(\Sigma n_e)}\frac{1}{\beta_e}. \tag{46}$$

The dispersion relation is expressed as

$$\begin{aligned}&D_+D_-D_\parallel+\mathcal{A}^2\{(R_+D_\parallel+R_{\parallel+}R_{+\parallel})D_--(R_-D_\parallel\\&\quad+R_{\parallel-}R_{-\parallel})D_+\}+\mathcal{A}^4\{(R_{+-}R_{-+}-R_+R_-)D_\parallel\\&\quad+R_{+-}R_{\parallel+}R_{-\parallel}+R_{-+}R_{\parallel-}R_{+\parallel}-R_-R_{\parallel+}R_{+\parallel}\\&\quad-R_+R_{\parallel-}R_{-\parallel}\}=0,\end{aligned} \tag{47}$$

in nondimensional variables suitable for numerical work.

The effect of damping, which will lead to thresholds for the excitation of parametric instabilities, can be included in the dispersion relation, Eq. (47), by replacing $X_{\pm j}^2$ by $X_{\pm j}(X_{\pm j}\pm i\overline{\nu_j})$ and $A_{\pm j}$ by $1-(\overline{m_j}/\overline{q_j})(X_{\pm j}\pm i\overline{\nu_j})$ in the definitions of $D_\pm$, Eq. (40), X_j^2 by $X_j(X_j+i\overline{\nu_j})$ in the definition of $D_\parallel$, Eq. (41), and $X_{\pm j}^2$ by $X_{\pm j}(X_{\pm j}\pm i\overline{\nu_j})$ in S_j, Eq. (45). The phenomenological collision frequency is also normalized to Ω_1, i.e., $\overline{\nu_j}=\nu_j/\Omega_1$. Naturally, this procedure is appropriate only as a first order correction because collisions are not taken into account in the terms that multiply powers of $\mathcal{A}$.

III. PARAMETRIC INSTABILITIES FOR A BEAM HEATED PLASMA

To discuss the solutions of the dispersion relation for a multicomponent plasma, let us take the example of a beam heated fusion plasma in a tokamak. We consider a plasma composed of deuterium (d), tritium (t), alpha particles (α), and two counter-streaming deuterium beams, which we denote by beam 1 and beam 2. We normalize all quantities to those of deuterium, which is therefore chosen as the reference species $j=1$ of the previous section. The calculations are carried out for numerical values close to the ones expected in an actual experiment, namely, $U_d=U_t=U_\alpha=0$, $|U_{\text{beam 1}}|=|U_{\text{beam 2}}|=0.2$, $\eta_d=\eta_t=1$, $\eta_\alpha=0.2$, $\eta_{\text{beam 1}}=\eta_{\text{beam 2}}=0.1$, $\beta_d=0.024$, $\beta_t=0.016$, $\beta_\alpha=0.5$, $\beta_{\text{beam 1}}=\beta_{\text{beam 2}}=0.01$, and $\beta_e=0.01$.

We assume that the pump wave is excited by some strong linear mechanism, such as by energetic particles in the case of toroidal Alfvén eigenmodes in a tokamak plasma, and that

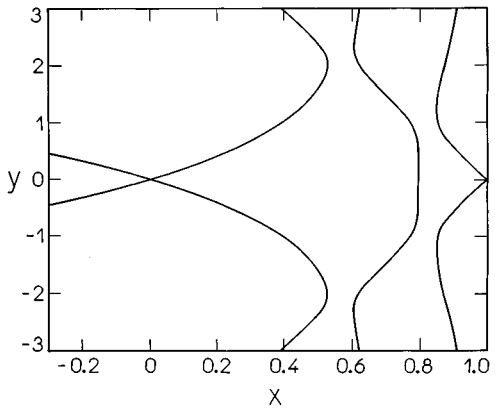

FIG. 1. Solution of the cold dispersion relation for waves propagating parallel to the magnetic field, Eq. (2), in a plasma with equal densities of deuterium and tritium, an α particle density equal to 0.2 relative to the deuterium density, and two counterstreaming deuterium beams with speeds equal to 0.2 times the Alfvén speed for deuterium, and density equal to 0.1 relative to the deuterium density.

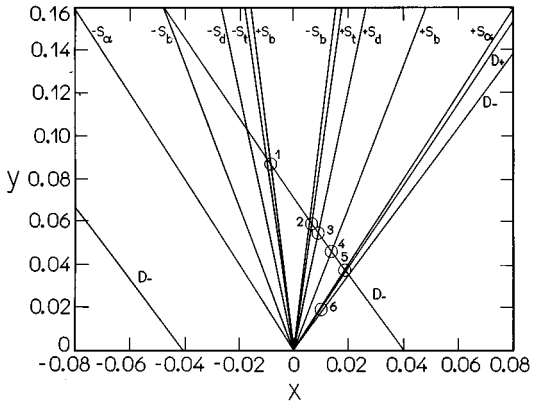

FIG. 2. Solution of the nonlinear dispersion relation, Eq. (39), for zero amplitude of the pump wave, and for $\beta_d=0.024$, $\beta_t=0.016$, $\beta_\alpha=0.5$, $\beta_{\text{beam }1}=\beta_{\text{beam }2}=0.01$. The origin of the diagram is at the frequency and wave number of the pump wave, $X_0=0.02$ and $Y_0=0.03582$. The values of the other parameters are the same of Fig. 1. The curves labeled S_j are the sound waves supported mainly by the α particles S_α, deuterium beams S_b, deuterium bulk ions S_d, and tritium S_t. The curves labeled D_+ and D_- are right and left circularly polarized waves, respectively. The intersections labeled 1 to 6 indicate the energetically favorable crossings.

linear damping is so weak that we can consider a constant amplitude pump wave. Actually, the TAE's are expected to be strongly damped only near the lower shear Alfvén continuum. Away from this limit, all damping mechanisms affect only the threshold value of the hot particle pressure gradient that excites the mode.

The solution of the collisionless ($\overline{v_j}=0$) linear dispersion relation for electromagnetic modes, Eq. (2), is plotted in Fig. 1. The curves in the first and fourth quadrants correspond to left-hand circularly polarized waves propagating forward and backward, respectively. In the second and third quadrants they become right-hand circularly polarized waves propagating backward and forward, respectively. The Alfvén waves correspond to the limit $X\ll 1$ along the branches crossing the origin. Without particle drifts, there should appear only two resonances, at $X=1$ for the deuterium and alpha species and at $X=2/3$ for the tritium species, and one stop band between the tritium resonance and the cutoff frequency, given by $Y=0$, $X\neq 0$. The Doppler shifted resonances of the drifting ions modify substantially this picture [12]. The stop band below the cutoff frequency shrinks somewhat and another one appears below the tritium resonance, as shown in Fig. 1. To investigate the parametric couplings, we choose a pump wave at the point $X_0=0.02$ and $Y_0=0.03582$ along the Alfvén branch.

The solutions of the nonlinear dispersion relation, Eq. (47), in the limit $\mathcal{A}\to 0$ for $\overline{\nu_j}=0$ are shown in Fig. 2. The graphical method of analysis is the one introduced in Ref. [18] (see also Refs. [13–15, 17]). The forward (backward) propagating sound waves are indicated by the symbols $+S_j$ $(-S_j)$ and the right and left circularly polarized waves are indicated by D_+ and D_-, respectively. The points numbered 1–6 represent the energetically favorable couplings between the different branches; they are all couplings between the D_- branch and diffrent sound waves, except crossing 6, which is between the D_+ and D_- branches. To find the crossings that give rise to parametric instabilities, we plot the solutions of the dispersion relation for $\mathcal{A}\neq 0$. The intersections that become a gap indicate complex roots of the dispersion relation occurring in conjugate pairs, i.e., instability. We find that the intersections labeled 1–6 give rise to instabilities; the first five lead to the excitation of a sound and an electromagnetic wave and the last one to an electromagnetic modulational instability [13,14]. This is an interaction between the pump and two electromagnetic sidebands mediated by a soundlike perturbation that is not an acoustic normal mode. It depends on coupling matrix elements that are quadratic with respect to the pump amplitude, in contrast with the other interactions that depend on matrix elements linear in the amplitude [see Eq. (34)] that couple the pump with one electromagnetic sideband and a sound mode. The gaps 2–5, for instance, are shown in Fig. 3 for $\mathcal{A}=0.1$. The complex roots across a gap can be readily evaluated and the maximum growth rate determined. The results are presented in Table I. The instability that results from the coupling to a sound wave supported mainly by the tritium species, gap 2,

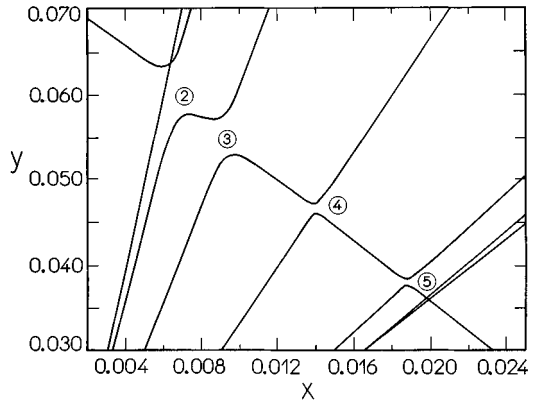

FIG. 3. Solution of the nonlinear dispersion relation, Eq. (47), showing the gaps that are formed at the intersections 2 to 5, for finite amplitude of the pump wave, i.e., $\mathcal{A}=B/B_z=0.1$. The values of the other relevant quantities are the same as in Figs. 1 and 2.

TABLE I. Maximum growth rates of the parametric instabilities for $\mathcal{A}=0.1$ and for the conditions of Figs. 2 and 3.

Crossing	Type	Frequency	Wave number	Growth rate
1	D_- ; S_{beam}	-9.6×10^{-3}	9.6×10^{-2}	7×10^{-5}
2	D_- ; S_t	6.8×10^{-3}	6×10^{-2}	10^{-3}
3	D_- ; S_d	9.2×10^{-3}	5.5×10^{-2}	8×10^{-4}
4	D_- ; S_{beam}	1.4×10^{-2}	4.6×10^{-2}	2×10^{-4}
5	D_- ; S_α	1.88×10^{-2}	3.78×10^{-2}	5×10^{-5}
6	D_- ; D_+	10^{-2}	1.8×10^{-2}	7×10^{-5}

has a very substantial growth rate, of the order of the real part of the frequency. The ones corresponding to the coupling to a sound wave supported mainly by the deuterium species and by the forward propagating deuterium beam have also considerable growth rates.

Naturally, our results depend on our choice of the parameters; in particular, a pump amplitude $\mathcal{A}=B/B_z=0.1$ is quite high, somewhat above the limit of what is realistically acceptable. However, calculating the maximum growth rate ω_i as a function of the pump intensity, we find $\omega_i\sim\mathcal{A}$, so that the growth rate for smaller pump amplitude can be readily estimated. This result is in agreement with the one obtained analytically for small values of the pump intensity in the single fluid MHD model [3], i.e.,

$$\omega_i=\frac{1}{2}\sqrt{\frac{\gamma\beta}{2}}k_0V_A\mathcal{A}. \tag{48}$$

In spite of the simplicity of our model, it is instructive to assess its consequences for actual experimental conditions. Let us, for instance, consider the experiment on the excitation of TAE modes by injection of an energetic deuterium beam in a deuterium plasma, carried out in DIII-D [19]. For the experimental parameters reported in Ref. [19], the Alfvén velocity is $v_A=2.2\times10^6$ m/s and the theoretical value for the real part of the mode frequency is $\omega_0=v_A/2qR\approx4.4\times10^5$ rad/s, where q is the safety factor and R is the major radius of the device (the experimental value is somewhat smaller and the mode spectrum is rather broad). Since in this case there is no tritium beam, we can consider only the sound waves supported by the deuterium species, which corresponds to crossing 3 in Table I. Recalling that, in our case, the frequencies are normalized to the cyclotron frequency of deuterium, and considering that $B\approx1$ T in the DIII-D experiment, it is easy to verify that the real frequency of this crossing is also 4.4×10^5 rad/s. The value of the linear growth rate of the TAE mode, γ_L, depends critically on the local value of the parameter β for the fast particles, which is difficult to determine precisely in an experiment. However, using the values of Table II of Ref. [19], we obtain $\gamma_L/\omega_0\sim10^{-2}$. We find that for a pump amplitude $\mathcal{A}\sim10^{-2}$ the growth rate of the parametric instability is of the same order of the linear growth rate predicted for the TAE instability. Therefore, one should expect that the parametric decay process sets a saturation on the mode amplitude of this order. However, this conclusion does not take into account the fact that in the presence of wave damping in the daughter waves, the parametric instability may have an amplitude

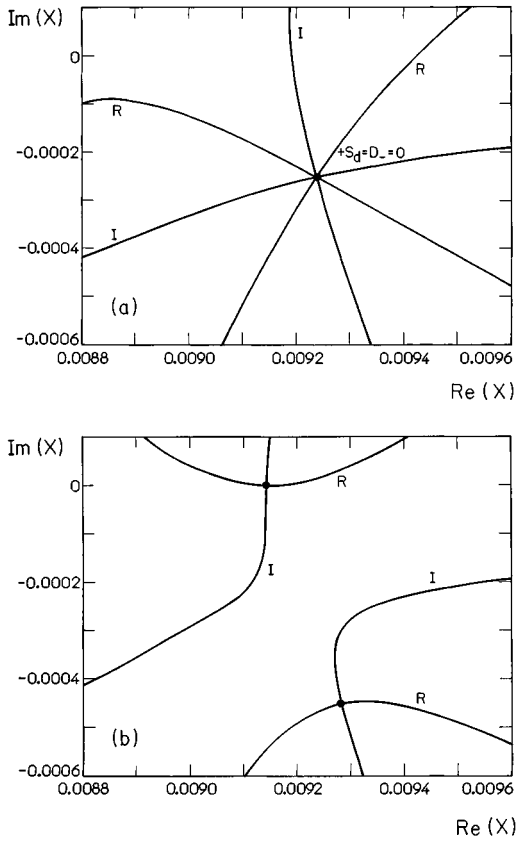

FIG. 4. Real and imaginary parts of the dispersion relation, Eq. (47), plotted in the Im(X) vs Re(X) diagram, for $Y=0.055$, $\overline{\nu}=5\times10^{-4}$, and $\mathcal{A}=0$ in (a), and $\mathcal{A}^2=8.8\times10^{-4}$ in (b). The double root $+S_d=D_-=0$ corresponds to crossing 3 of Fig. 2.

threshold. As we shall see, the threshold effect is important and depends on whether the electromagnetic daughter wave is stable or unstable.

In order to calculate the thresholds for the parametric instabilities, we include the collision frequencies in the linear part of the dielectric tensor, as discussed at the end of the previous section. The calculational procedure is as follows. First we fix the values of the collision frequencies and of the normalized wave number Y at a given crossing of Fig. 2. The curves corresponding to the real and imaginary parts of the dispersion relation are then plotted in a Im(X) versus Re(X) diagram; the roots of the dispersion relation are given by the crossings of the two curves. In Fig. 4 we show such plots for $Y=0.055$ and $\overline{\nu}=5\times10^{-4}$. In reality, the sound waves in an infinite plasma for our conditions are heavily damped and a larger value of the collision frequency should be taken for them. However, we have chosen this value taking into account that in an actual experiment the damping is substantially reduced by the presence of a net plasma current. The value of Y is the one at the crossing labeled 3 in Fig. 2, for $X=9.2\times10^{-3}$. We see in Fig. 4(a) drawn for $\mathcal{A}=0$, that there is a double root $+S_d=D_-=0$ with negative imaginary part, corresponding to damping introduced by collisions. Increasing the value of the pump, we can determine the threshold value, $\mathcal{A}_{\text{thr}}$, for which a solution of the dispersion relation with a positive imaginary part starts to appear, as shown in Fig. 4(b) for $\mathcal{A}^2=8.8\times10^{-4}$. The double root $+S_d=D_-=0$

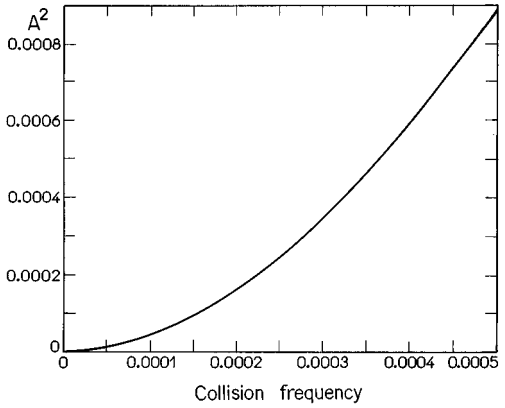

FIG. 5. Value of the threshold of the square of the pump amplitude as a function of the collision frequency for the parametric decay labeled 3 in Table I.

is split into two roots, one with a slightly positive imaginary part, indicating instability. Following this procedure, we can determine the value of the threshold as a function of the collision frequency for all instabilities listed in Table I. In Fig. 5 we show the result for coupling 3, which has one of the largest growth rates in the absence of collisions. The curve can be fitted by a second order polynomial, $\mathcal{A}_{\rm thr}^2 = 0.284\overline{\nu} + 3038\overline{\nu^2}$. From the single fluid model, in the limit of small collision frequency [3], one obtains $\mathcal{A}_{\rm thr} \sim \overline{\nu}$. Thus, our calculations indicate that the single fluid model result is valid only for normalized collision frequencies $\overline{\nu} \gtrsim 10^{-3}$. Since the electromagnetic and sound waves could have different damping rates, one may consider the possibility of different collision frequencies in the model. From estimates for simple parametric decay processes, one expects the threshold amplitude to be proportional to the geometric mean of the collision frequencies. To check this ansatz in a multifluid plasma, we have calculated the value of the threshold amplitude as a function of the collision frequency of the electromagnetic daughter waves, $\overline{\nu_D}$, for a fixed value of the collision frequency of the sound wave, $\overline{\nu_s} = 5 \times 10^{-4}$. We find that $\mathcal{A}_{\rm thr}^2 = 0.015\sqrt{\overline{\nu_D}} + 1.70\overline{\nu_D}$, showing that the expected behavior is valid for large collision frequencies, as before.

Moreover, one also has to consider the possibility that the electromagnetic daughter wave is another unstable TAE mode [9,10]. This situation can be simulated by assuming a negative collisional frequency for one branch. In this case, there is no threshold, even taking into account damping of the sound waves. In the case of the modulational instability, crossing 6 of Fig. 2 at $(X,Y) = (0.010, 0.018)$, and taking $\mathcal{A} = 0.1$, we find that in the absence of damping ($\overline{\nu} = 0$) there is a coupling between D_+ and D_- with a growth rate $\gamma = 7 \times 10^{-5}$. When damping $\overline{\nu} = 5 \times 10^{-4}$ is introduced the instability is quenched, since the threshold for $\mathcal{A}$ is very high ($\mathcal{A} > 0.35$). Nevertheless, when a daughter wave is an unstable mode, the threshold vanishes, thus allowing for the development of the instability for infinitesimal values of $\mathcal{A}$. For the TAE modes, the main damping mechanism is coupling to the continuum. From the analysis of this process by Rosenbluth *et al.* [20] and considering a parabolic profile for the inverse rotational transform, we find that for a typical case of a mode with poloidal mode number $m = 4$, the ratio of the damping rate to the real frequency is of the order of 2%. This value would correspond to a significant phenomenological collision frequency in our model, giving $\mathcal{A}_{\rm thr} \approx 10^{-2}$ for the parametric decay of TAE's by coupling to sound waves to occur. However, as pointed out above, when the coupling is with an excited TAE sideband wave, there should be no threshold for the instability.

IV. DISCUSSION AND CONCLUSIONS

We have presented an analysis of the parametric decay of cyclotron waves propagating parallel to the magnetic field in multi component plasmas, including the effect of collisions, which can be relevant for astrophysical and fusion plasmas. We have explicitly shown that in the low frequency range considered, the presence of drifting motions of subsets of the total electron population does not influence the nonlinear (nor the linear) dispersion relation if the electric current is zero, although the effect of possible temperature differences between electron groups remains. The nonlinear dispersion relation for EICW, which has been presented in nondimensional form ready for numerical applications, is enriched by many new roots associated with the presence of multi-ion species and their possible drifts. It is important to observe that each ion species provides two new sound branches, and that each sound branch may open a new channel for energy transfer from the pump to the daughter waves. Moreover, the sound speed of these acoustic branches is modified by the corresponding drift of the ion species. In the presence of a finite pump amplitude the sound propagation is modified further as shown by Eqs. (18) and (33). This effect has been noted in Ref. [14], where an example of a pump induced coupling is presented (see Figs. 13 and 14 of Ref. [14]). It is a crossing of a sound branch and an EICW mode that exists only when the pump amplitude is above a certain value ($\mathcal{A}$ near 0.1 in the example of Ref. [14]), and produces a parametric instability for larger values of $\mathcal{A}$.

The form of the equations for the nonlinear couplings, Eqs. (28), (30), and (32), is more convenient than the one provided for two ion species in Refs. [13–15] and [17] not only because the extension to more than two ion components becomes cumbersome following the procedure described there, but mainly because in the present formulation, with the linear dielectric components of the waves clearly in evidence, we can easily introduce heuristic modifications in the dispersion relation. Hence, we have been able to introduce collisions in the linear dielectric terms that simulate the effects of wave damping, so that the amplitude threshold of the instability can be evaluated for any chosen wave coupling.

The important case of a fusion plasma heated by neutral beam injection has been analyzed in detail. Because in our analysis we assume a circularly polarized wave propagating in a homogeneous multifluid current-free plasma, our results have to be considered only as a first step in understanding the effect of multiion species and damping on the parametric decay of toroidal Alfvén eigenmodes in fusion plasmas. Naturally, tokamak plasmas are not current free. If one includes a net current in a infinite homogeneous plasma, there appears an instability for values of the wave number perpendicular to the equilibrium magnetic field tending to zero and

very low frequencies [23]. However, this instability does not appear in a finite inhomogeneous plasma because of the boundary conditions and thus we consider a current free plasma to eliminate this spurious effect. The question of polarization is more subtle. The TAE modes are global discrete eigenmodes that exist in gaps of the shear Alfvén continuum, produced by toroidal coupling [24]. Therefore, they exist only in toroidal geometry and one is faced with the question of how to simulate their main characteristics, viz., polarization, in a simple homogeneous plasma model. In the slab model approximation to toroidal geometry, the TAE's are linearly polarized shear Alfvén waves with $k_\perp \ll k_\parallel$, and the eigenfunctions are strongly peaked in the radial direction [25]. If linearly polarized waves are considered in the homogeneous model, there appear new couplings with longitudinal perturbations caused by the ponderomotive effect due to the Lorentz force. However, to simulate the peakedness of the TAE eigenfunction, one would have to sum over many modes and with different values of $k_\perp$ and probably these couplings would average out. This difficult problem is avoided by considering circularly polarized waves. Furthermore, in real toroidal geometry, the shear Alfvén waves are not purely linearly polarized because of the variation of the Alfvén speed in a magnetic surface [26] and the parametric couplings that occur only for pure linear polarization should not be relevant for these waves.

The multi-ion species model shows that there are five parametric instabilities for the pump with five possible acoustic modes. The most important ones, as far as growth rates are concerned, are those related with the deuterium, tritium, and beam sounds, all forward propagating (crossings 2, 3, and 4 of Table I). Our calculation gives an estimate of the decay of a single excited Alfvén by coherent parametric coupling of sideband waves and ion sound. Thus, it complements the work of other authors [9–11] in the sense that they have considered other possible saturation mechanisms. It was shown that if all product waves are damped, there is a threshold on the pump amplitude for parametric decay, as expected. However, in a scenario relevant to the TAE mode, one has to consider the possibility of an unstable electromagnetic daughter wave, in which case the parametric instability is triggered without threshold. These results points toward the interest of extending this analysis, including the evaluation of the threshold, and the presence of several acoustic branches, in a more realistic model of the TAE modes (with radial dependence and toroidicity effects) and their nonlinear couplings, a task, however, not likely to be trivial.

ACKNOWLEDGMENTS

This work has been partially supported by grant PID-BID No. 0594/92 and FONDECYT Grant No. 1940360. We also want to acknowledge support from Instituto de Física del Plasma, Consejo Nacional de Investigaciones Científicas y Técnicas (Argentina), Fundación Andes (Chile), Fundação de Amparo à Pesquisa do Estado de São Paulo, and Conselho Nacional de Desenvolvimento Científico e Tecnológico (Brasil).

[1] A. A. Galeev and V. N. Oraevskii, Dokl. Akad Nauk SSSR **147**, 71 (1962) [Sov. Phys. Dokl **7**, 988 (1963)].
[2] Y. C. Lee and P. K. Kaw, Phys. Fluids **15**, 911 (1972).
[3] C. N. Lashmore-Davies, Phys. Fluids **19**, 587 (1976).
[4] A. Hasegawa and L. Chen, Phys Fluids **19**, 1924 (1976).
[5] P. K. Shukla, M. Y. Yu, and L. Stenflo, Phys. Scr. **34**, 169 (1986).
[6] C. S. Liu and V. K. Tripathi, Phys. Rep. **130**, 143 (1986)
[7] H. Bigliari and P. H. Diamond, Phys. Fluids B **4**, 3009 (1992).
[8] F. Y. Gang, Phys. Fluids B **4**, 3152 (1992).
[9] T. S. Hahm and L. Chen, Phys. Rev. Lett. **74**, 266 (1995).
[10] F. Y. Gang and J.-N. Leboeuf, Phys. Fluids B **5**, 2736 (1993).
[11] G. Vlad, C. Kar, F. Zonca, and F. Romanelli, Phys. Plasmas **2**, 418 (1995).
[12] L. Gomberoff and R. Elgueta, J. Geophys. Res. **96**, 9801 (1991).
[13] J. V. Hollweg, R. Esser, and V. Jayanti, J. Geophys. Res. **98**, 3491 (1993).
[14] L. Gomberoff, F. T. Gratton, and G. Gnavi, J. Geophys. Res. **99**, 717 (1994).
[15] L. Gomberoff, F. T. Gratton, and G. Gnavi, J. Geophys. Res. **100**, 1871 (1995).
[16] J. V. Hollweg, J. Geophys. Res. **99**, 23 431 (1994).
[17] R. M. O. Galvão, G. Gnavi, L. Gomberoff, and F. Gratton, Plasma Phys. Controlled Fusion Res. **36**, 1679 (1994).
[18] M. Longtin and B. U. Ö. Sonnerup, J. Geophys. Res. **91**, 6816 (1986).
[19] W. W. Heidbrink, E. J. Strait, E. Doyle, G. Sager, and R. T. Snider, Nucl. Fusion **31**, 1635 (1991).
[20] M. N. Rosenbluth, H. L. Berk, J. W. Van Dam, and D. M. Lindberg, Phys. Rev. Lett. **68**, 596 (1992).
[21] W. W. Heidbrink, E. J. Strait, M. S. Chu, and A. D. Turnbull, Phys. Rev. Lett. **71**, 855 (1993).
[22] E. J. Strait, W. W. Heidbrink, and A. D. Turnbull, Plasma Phys. Control. Fusion Res. **36**, 1211 (1994).
[23] R. Cross, *An Introduction to Alfvén Waves* (Adam Hilger, Bristol, 1988).
[24] D. A. D'Ippolito and J. P. Goedbloed, Plasma Phys. **22**, 1091 (1980).
[25] C. Z. Cheng, L. Chen, and M. S. Chance, Ann. Phys. (N.Y.) **161**, 21 (1984).
[26] J. P. Goedbloed, Phys. Fluids **18**, 1258 (1975).